Elastic response of $U_3Cu_4Ge_4$ to spontaneous and field-induced phase transitions

Gorbunov, D.; Hibino, R.; Scurschii, I.; Yanagisawa, T.; Andreev, A. V.; Zherlitsyn, S.; Wosnitza, J.;

Originally published:

October 2022

Physical Review B 106(2022), 144403

DOI: https://doi.org/10.1103/PhysRevB.106.144403

Elastic response of $U_3Cu_4Ge_4$ to spontaneous and field-induced phase transitions

D. I. Gorbunov,[1] R. Hibino,[2] Y. Skourski,[1] T. Yanagisawa,[2] A. V. Andreev,[3] S. Zherlitsyn,[1] and J. Wosnitza[1,4]

[1]*Hochfeld-Magnetlabor Dresden (HLD-EMFL) and Würzburg-Dresden Cluster of Excellence ct.qmat, Helmholtz-Zentrum Dresden-Rossendorf, 01328 Dresden, Germany*
[2]*Department of Physics, Hokkaido University, Sapporo 060-0810, Japan*
[3]*Institute of Physics, Academy of Sciences, Na Slovance 2, 182 21 Prague, Czech Republic*
[4]*Institut für Festkörper- und Materialphysik, Technische Universität Dresden, 01062 Dresden, Germany*

$U_3Cu_4Ge_4$ is a uniaxial ferromagnet that displays a first-order magnetization process (FOMP) at 25 T for field applied along the hard b axis. Here, we report on ultrasound and magnetostriction measurements of $U_3Cu_4Ge_4$ in static and pulsed magnetic fields up to 40 T. The FOMP causes step-wise anomalies in the magnetoelastic properties. $U_3Cu_4Ge_4$ elongates along the a and c axes and shrinks along the b axis, leading to an almost zero volume effect. The sound velocities of the longitudinal and transverse acoustic waves decrease sharply at the FOMP, whereas the sound attenuation shows pronounced peaks. An analysis of the ultrasound data using a mean-field theory suggests the existence of quadrupolar interactions and crystal-electric-field effects. The $5f$ electronic states are between itinerant and localized, typical of uranium-based intermetallic compounds.

I. INTRODUCTION

Uranium-based intermetallic compounds are characterized by extended $5f$ electronic states. The $5f$ wavefunctions are intermediate between itinerant and localized and resemble in some characteristic features those of the d states of transition metals, rather than the localized $4f$ states of lanthanides. This has significant consequences for uranium-based materials. First, their electronic properties can be significantly affected by external variables such as magnetic field, pressure, and elemental substitution (see, e.g., Refs. [1, 2]). Second, the dominance of many-body phenomena in this crossover regime gives rise to exotic states, e.g., unconventional superconductivity that coexists with antiferromagnetic or ferromagnetic order [3–7].

For uranium magnetism, another important aspect is the strong spin-orbit interaction that couples the magnetic moments and both the crystal and electronic structures. Directional bonding of the $5f$ states gives rise to a large hybridization-induced magnetocrystalline anisotropy, the energy of which is usually inaccessible by common experimental methods [8–10]. Recently, $U_3Cu_4Ge_4$ was found to be an exception to this rule as it provides a convenient tool to quantify its large magnetic-anisotropy energy [11].

$U_3Cu_4Ge_4$ crystallizes in an orthorhombic crystal structure of $Gd_3Cu_4Ge_4$ type (space group $Immm$, no. 71), where the U atoms occupy two inequivalent crystallographic positions [inset of Fig. 1(a)]. $U_3Cu_4Ge_4$ displays ferromagnetic order with a Curie temperature of T_C = 67-73 K [11–14]. The U magnetic moments of 1.71 μ_B align along the a axis which is the shortest dimension of the crystal structure [14]. $U_3Cu_4Ge_4$ shows a first-order magnetization process (FOMP) for field applied along the hard b axis [11]. The transition can be modeled using a phenomenological theory, which yields anisotropy constants up to the sixth order [11, 15].

A FOMP occurs due to the existence of two inequivalent minima in the magnetic-anisotropy energy of a material corresponding to two distinct directions of the magnetization vector [15, 16]. A FOMP is a phase transition changing the anisotropy that likely affects the $5f$ states of $U_3Cu_4Ge_4$ due to the hybridization-induced magnetocrystalline anisotropy. Therefore, one may expect pronounced lattice instabilities at the FOMP related to, e.g., changes in the $5f$ localization and/or multipolar interactions.

Here, we report on high-field ultrasound and magnetostriction measurements of $U_3Cu_4Ge_4$. We find large anomalies in the sound velocity and sound attenuation at the FOMP, which signals a strong magnetoelastic coupling. $U_3Cu_4Ge_4$ also shows pronounced magnetostrictions at the field-induced transition, whereas the volume change is close to zero. The negligible volume effect suggests a constant degree of $5f$-electron localization across the FOMP. The observed lattice instability, concomitant with rotating uranium magnetic moments, reflects the large spin-orbit coupling of uranium. Additionally, some longitudinal acoustic waves show a dispersion as a function of temperature, most likely due to rattling motions of the Cu and/or Ge atoms.

II. EXPERIMENTAL DETAILS

We used a $U_3Cu_4Ge_4$ single crystal from the same batch as reported in Ref. [11]. Back-scattered Laue diffraction was used to orient the crystal for ultrasound and magnetostriction measurements.

The magnetic susceptibility was measured between 2 and 300 K using a commercial Physical Property Measurement System. We applied an ac-excitation field of 1 mT along the a axis at a frequency of 77 Hz.

Relative sound-velocity changes and sound attenuation were measured using a phase-sensitive pulse-echo ultrasound technique [17, 18]. A pair of piezoelectric transducers were glued to opposite surfaces of the single crystal in order to excite and detect acoustic waves. We measured the longitudinal, C_{33} ($\boldsymbol{k} \parallel \boldsymbol{u} \parallel c$), and transverse, C_{44}

($\boldsymbol{k} \parallel c, \boldsymbol{u} \parallel b$) and C_{55} ($\boldsymbol{k} \parallel c, \boldsymbol{u} \parallel a$), acoustic modes. Here, $\boldsymbol{k}$ and $\boldsymbol{u}$ are the wave vector and polarization of the acoustic waves, respectively. Absolute values of the sound velocity are $v_{33} = [4540 \pm 100]$ m/s, $v_{44} = [2090 \pm 100]$ m/s, and $v_{55} = [2430 \pm 100]$ m/s at 4.2 K. The elastic modulus, C_{ii}, can be computed using the relation $C_{ii} = \rho v_{ii}^2$, where $\rho = 10.67 \times 10^3$ kg/m^3 is the mass density of $U_3Cu_4Ge_4$.

Magnetostriction measurements were performed using the fiber Bragg grating (FBG) technique [19]. A standard telecommunication fiber with 1 mm FBG and a peak reflectivity at 1550 nm was glued to the surface of the sample. The strain-dependent shift of the peak is detected using a high-resolution spectrometer with a camera operating at 47 kHz. For field applied along the b axis, we measured the longitudinal, $\Delta l/l_b$, and transverse magnetostriction along the a and c axes, $\Delta l/l_a$ and $\Delta l/l_c$, respectively.

III. RESULTS

The magnetic susceptibility, χ, of $U_3Cu_4Ge_4$ for an excitation field of 1 mT applied along the easy a direction shows a large maximum at $T_C = 73$ K as the system enters the ferromagnetic state [Fig. 1(a)]. The relative sound velocities, $\Delta v/v$, for the acoustic modes C_{33} and C_{55} show distinct anomalies at T_C and increase with decreasing temperature in zero field [Fig. 1(b)]. A small upturn is observed for the C_{33} mode around 20 K. The acoustic mode C_{44} softens with decreasing temperature with again a distinct anomaly at T_C. Below 40 K, the sound velocity for this mode displays large changes of $\approx$ 1%. A sharp minimum is seen just above 20 K, in the same temperature range where $\Delta v/v$ for C_{33} displays an upturn. The sound attenuation, $\Delta\alpha$, shows maxima near 20 K for the modes C_{33} and C_{44} [Fig. 1(c)]. The attenuation is especially large, 100 dB/cm, for C_{44}. Except for $\Delta\alpha$ of C_{55}, that displays a small jump at T_C, we cannot resolve anomalies at the Curie temperature in $\Delta\alpha$ for C_{33} and C_{44} in zero field.

To determine whether the origin of the anomalies observed in $\Delta v/v$ and $\Delta\alpha$ is magnetic, we performed ultrasound measurements in magnetic fields applied along the b direction of $U_3Cu_4Ge_4$. The anomalies in the elastic properties in the vicinity of the Curie temperature become more pronounced with increasing field. The sound velocity for C_{33} develops a minimum in fields between 10 and 13 T [Fig. 2(a)]. The minimum changes to a step-like anomaly at 17 T. $\Delta v/v$ for C_{44} shows a minimum that sharpens [Fig. 2(b)]. The sound velocity for C_{55} shows a step-like feature [Fig. 2(c)].

For all acoustic modes, the sound attenuation develops maxima at the ferromagnetic-paramagnetic transition with increasing field [Figs. 2(d), (e), and (f)]. The maximum in $\Delta\alpha$ has a fine structure for C_{55} in fields above 10 T [Fig. 2(f)]. Interestingly, the anomalies observed in $\Delta v/v$ and $\Delta\alpha$ near 20 K for C_{33} and C_{44} do not change with field. This evidences that they have a nonmagnetic origin.

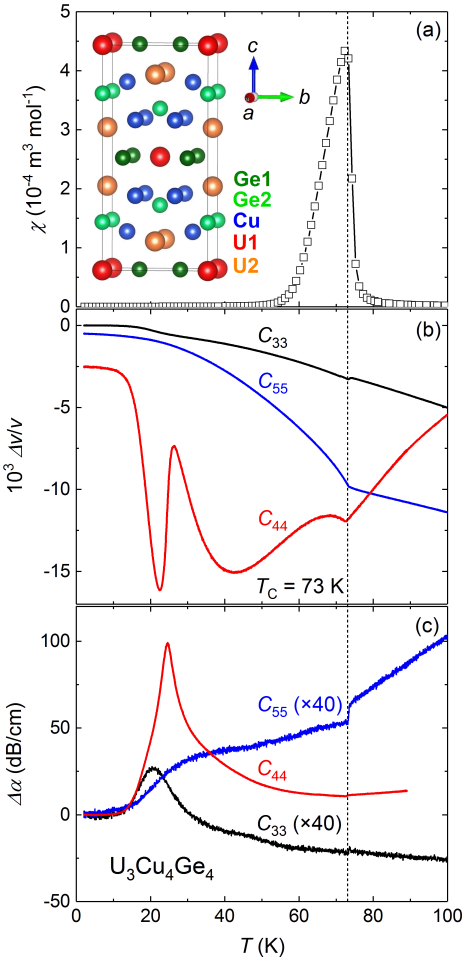

FIG. 1: Temperature dependences of (a) the magnetic susceptibility, χ, for an excitation field of 1 mT applied along the a axis; (b) the relative sound-velocity changes, $\Delta v/v$; and (c) the sound attenuation, $\Delta\alpha$, for the longitudinal, C_{33}, and transverse, C_{44} and C_{55}, acoustic modes for $U_3Cu_4Ge_4$. The $\Delta v/v$ curves are vertically offset for clarity. The $\Delta\alpha$ values for C_{33} and C_{55} are scaled by a factor of 40. The ultrasound frequencies were 34.7, 17.1, and 30.6 MHz for the acoustic modes C_{33}, C_{44}, and C_{55}, respectively. The inset in panel (a) shows the crystal structure of $U_3Cu_4Ge_4$.

We performed ultrasound measurements at various frequencies for the acoustic mode C_{33}. Near 20 K, the shoulder-like anomaly in $\Delta v/v$ and the maximum in $\Delta\alpha$ shift to higher temperatures when the ultrasound frequency increases from 34.7 to 168.2 MHz [Figs. 3(a) and (c)]. Additionally, the absolute values of the sound attenuation increase with frequency. The $\Delta v/v$ vs. T and $\Delta\alpha$ vs. T dependences can be described phenomenologically using a Debye-type dispersion [20, 22, 23]:

$$v^2 = v_0^2 \left[1 + \frac{v_\infty^2 - v_0^2}{v_0^2} \cdot \frac{\omega^2\tau^2}{1+\omega^2\tau^2}\right], \qquad (1)$$

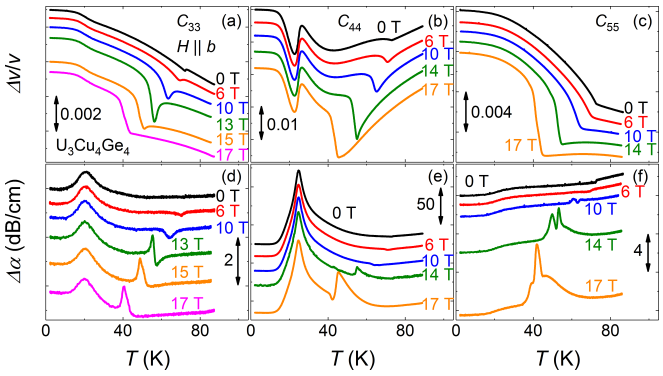

FIG. 2: Temperature dependences of (a), (b), (c) the relative sound-velocity changes, $\Delta v/v$, and (d), (e), (f) the sound attenuation, $\Delta\alpha$, for the longitudinal, C_{33}, and transverse, C_{44} and C_{55}, acoustic modes, respectively, for field applied along the b axis of $U_3Cu_4Ge_4$. The curves are vertically offset for clarity. The ultrasound frequencies were 34.7, 17.1, and 30.6 MHz for the acoustic modes C_{33}, C_{44}, and C_{55}, respectively.

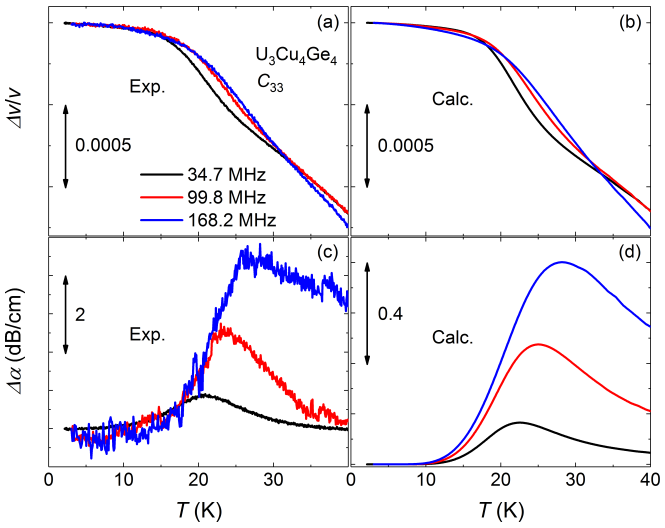

FIG. 3: Experimental and calculated temperature dependences of (a), (b) the relative sound-velocity changes, $\Delta v/v$, and (c), (d) the sound attenuation, $\Delta\alpha$, for the longitudinal acoustic mode C_{33} of $U_3Cu_4Ge_4$. The ultrasound frequencies were 34.7, 99.8, and 168.2 MHz.

$$\alpha = \frac{v_\infty^2 - v_0^2}{2v_0^3} \cdot \frac{\omega^2\tau}{1+\omega^2\tau^2}, \qquad (2)$$

where v_∞ and v_0 are the background velocities in the high- and low-frequency limit, $\tau = \tau_0 \exp(\frac{E}{T})$, τ_0 is the relaxation time, E is the activation energy, and $\omega = 2\pi f$ is the angular frequency. We assumed $v_0 = aT^2 + bT^4 + cT^6$ and $v_\infty = v_0 + \Delta v$. Our fits are in very good quantitative agreement for the sound velocity [Fig. 3(b)] and reasonable agreement for the sound attenuation [Fig. 3(d)] and led to the values $\tau_0 = 40$ ps and $E = 95$ K. These values are similar to those of some filled skutterudites, $R\mathrm{Os_4Sb_{12}}$ and $R\mathrm{Fe_4Sb_{12}}$ (R is a rare-earth element) [23, 24], and the clathrate $\mathrm{Ce_3Pd_{20}Ge_6}$ [25]. It is known that ultrasonic attenuation obtained phenomenologically is usually smaller than that observed in experiment [24, 26].

We propose that the dispersion observed for C_{33} around 20 K is due to rattling motions, i.e., thermally activated off-center ionic motion in a multi-well potential. For filled skutterudites and clathrates, the rattling motion is attributed to the heavy rare-earth atoms due to the caged structure of these materials. $U_3Cu_4Ge_4$ has no caged structure and our analysis shows that the off-center configuration relates to either the Ge or Cu atoms. According to our calculations, the Ge1 ($4h$ site) and Ge2 ($4i$ site) atoms have the largest free space for vibration at room temperature [27], 1.7721 Å and 1.6251 Å, respectively, while their isotropic displacements are about 0.0030 Å^2 [11]. Cu, on the other hand, has less free space for vibration, 0.5629 Å, but it is the lightest atom in $U_3Cu_4Ge_4$ and shows the largest isotropic displacement, 0.0062 Å^2.

Next, we study the elastic response of $U_3Cu_4Ge_4$ to the first-order magnetization process (FOMP). In the magnetization, the FOMP is observed as a jump at 25 T and 2 K for field applied along the hard b axis [Fig. 4(a)]. The field-induced transition is accompanied by a positive transverse magnetostriction jump of $\Delta l/l_a = 1.6(2) \times 10^{-4}$ and $\Delta l/l_c = 3.0(2) \times 10^{-4}$ along the a and c axes, respectively. The anomaly along the a

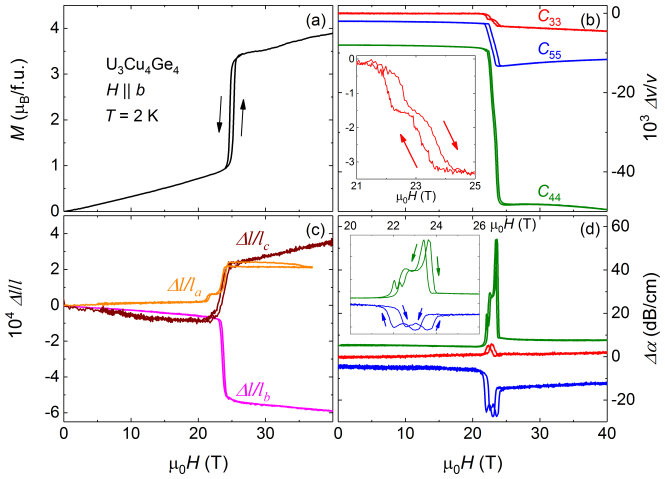

FIG. 4: Field dependences of (a) the magnetization, M; (b) the relative sound-velocity changes, $\Delta v/v$; (c) the linear magnetostriction, $\Delta l/l$, along the a, b, and c axes; and (d) the sound attenuation, $\Delta\alpha$, for the longitudinal, C_{33}, and transverse, C_{44} and C_{55}, acoustic modes for field applied along the b axis of $U_3Cu_4Ge_4$ at 2 K. In panels (b) and (d), the curves are vertically offset for clarity. The insets in panels (b) and (d) show $\Delta v/v$ for C_{33} and $\Delta\alpha$ for C_{44} and C_{55}, respectively, in the vicinity of the FOMP. The ultrasound frequencies were 38.4, 57, and 92 MHz for the acoustic modes C_{33}, C_{44}, and C_{55}, respectively.

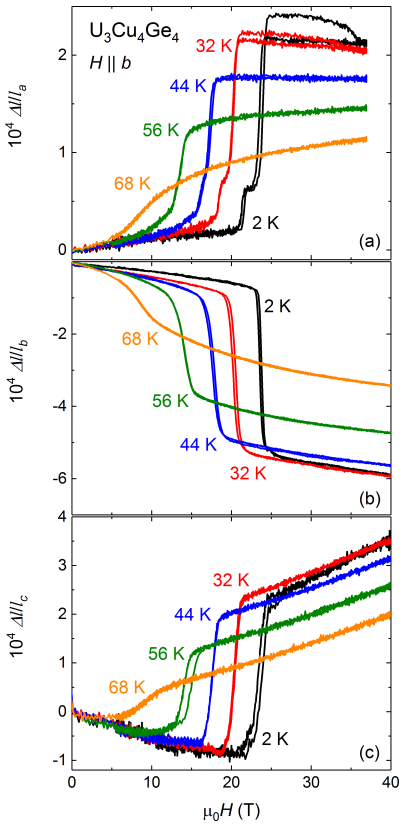

FIG. 5: Field dependences of the magnetostriction, (a) $\Delta l/l_a$, (b) $\Delta l/l_b$, and (c) $\Delta l/l_c$, along the a, b, and c axes for field applied along the b axis of $U_3Cu_4Ge_4$ at selected temperatures.

axis is preceded by a small step at 22 T. Along the b axis, a lattice contraction, $\Delta l/l_b = -4.2(2)\times10^{-4}$, is observed. Thus, the volume magnetostriction, $\Delta l/l_a+\Delta l/l_b+\Delta l/l_c$, is close to zero at the FOMP.

The sound velocity decreases at the transition for all measured acoustic modes [Fig. 4(b)]. $\Delta v/v$ for C_{33} shows a two-step anomaly [inset in Fig. 4(b)]. The softening is especially large, $\approx$ 4%, for C_{44}. We also found pronounced anomalies in the sound attenuation at the FOMP [Fig. 4(d)]. Here, the largest peak in $\Delta\alpha$, 50 dB/cm, is also observed for C_{44}. $\Delta\alpha$ for C_{55} is negative at the FOMP, i.e., acoustic waves intensify at the phase transition. Enlarged views of $\Delta\alpha$ vs. H reveal several features for C_{44} and C_{55} in the vicinity of the FOMP [inset in Fig. 4(d)].

With increasing temperature, the critical field of the FOMP decreases as evidenced by our magnetostriction and ultrasound measurements (Figs. 5 and 6). We observe shrinking anomalies in $\Delta l/l_a$, $\Delta l/l_b$, and $\Delta l/l_c$, whereby their step-wise character takes on a more continuous nature [Figs. 5(a), (b), and (c)]. The double step in $\Delta l/l_a$ can be resolved up to 44 K [Fig. 5(a)].

Our ultrasound data reveal more substantial changes in the character of the transition at elevated temperatures. The step-wise anomaly in the sound velocity for

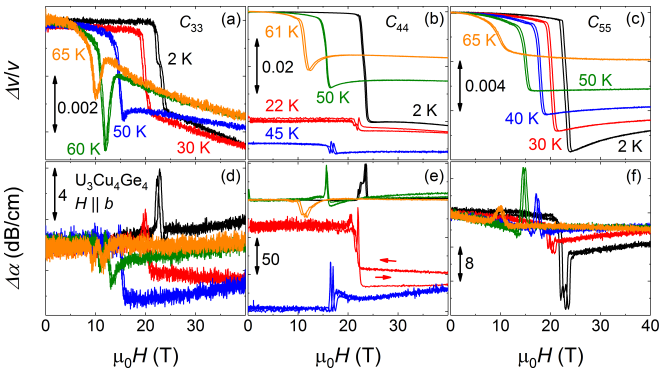

FIG. 6: Field dependences of (a), (b), (c) the relative sound-velocity changes, $\Delta v/v$, and (d), (e), (f) the sound attenuation, $\Delta\alpha$, for the longitudinal, C_{33}, and transverse, C_{44} and C_{55}, acoustic modes, respectively, for field applied along the b axis of $U_3Cu_4Ge_4$ at selected temperatures. In panels (b) and (e), some curves are vertically offset for clarity. The ultrasound frequencies were 38.4, 57, and 92 MHz for the acoustic modes C_{33}, C_{44}, and C_{55}, respectively.

C_{33} turns into a sharp minimum above 50 K [Fig. 6(a)]. This is accompanied by a reduction of the peak in the sound attenuation [Fig. 6(d)]. The step in $\Delta v/v$ for C_{44} decreases in height and also turns into a minimum with increasing temperature [Fig. 6(b)], while $\Delta\alpha$ decreases at 61 K [Fig. 6(e)]. For this acoustic mode, the results are strongly affected by the large attenuation around 20 K [see Fig. 1(c)]. At 22 and 45 K, we observe a much smaller effect in the sound velocity and step-like anomalies with narrow peaks in the sound attenuation, unlike the results at 2, 50, and 61 K. This might be an artifact due to the rattling motion [28]. For C_{55}, the softening at the FOMP gradually decreases with temperature [Fig. 6(c)]. $\Delta\alpha$, however, goes from a minimum to a maximum at the phase transition [Fig. 6(f)].

The phase diagram of $U_3Cu_4Ge_4$ for field applied along the b axis shows an extended region between 23 and 25 T separating the ferromagnetic and paramagnetic phases (Fig. 7). This reflects the first-order nature of the FOMP with several anomalies observed in the magnetostriction, sound velocity, and attenuation. This might indicate that either the FOMP occurs at slightly different fields in various parts of the single crystal or the FOMP is a multistep process. The phase diagram also shows a region where we observe ultrasonic dispersion in the C_{33} and C_{44} data. Although the dispersion is of nonmagnetic origin, it would be interesting to see if it changes across the ferromagnetic-paramagnetic phase transition. This requires ultrasound measurements in static fields above 25 T.

IV. DISCUSSION

The strong magnetoelastic coupling of $U_3Cu_4Ge_4$ is reflected in the pronounced anomalies observed in our mag-

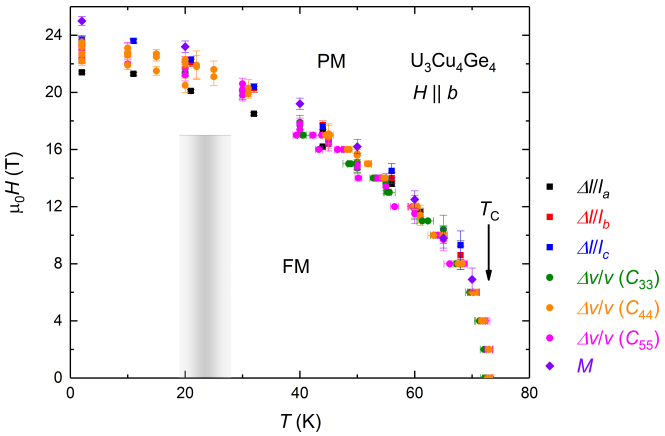

FIG. 7: Phase diagram of $U_3Cu_4Ge_4$ for field applied along the b axis. The gray region shows the temperature-field window where ultrasonic dispersion is observed in the static-field measurements.

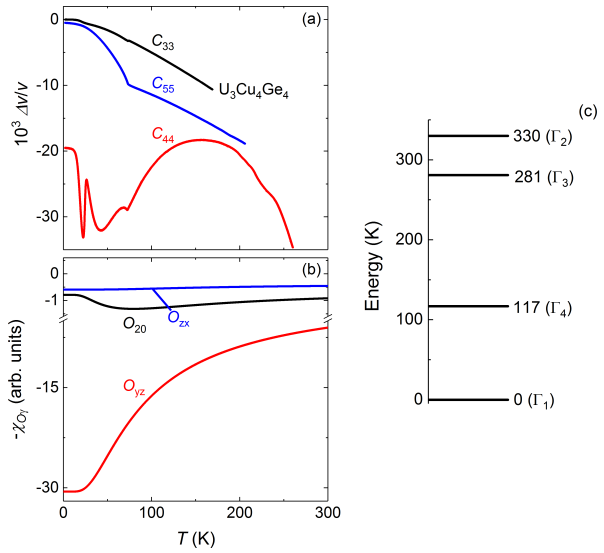

FIG. 8: Temperature dependences of (a) the relative sound-velocity changes, $\Delta v/v$, for the longitudinal, C_{33}, and transverse, C_{44} and C_{55}, acoustic modes for $U_3Cu_4Ge_4$ and (b) calculated quadrupolar susceptibility, $-\chi_{O_\gamma}$, for the quadrupolar operators O_{20}, O_{yz}, and O_{zx}. The ultrasound frequencies were 34.7, 17.1, and 30.6 MHz for the acoustic modes C_{33}, C_{44}, and C_{55}, respectively. (c) CEF level scheme of a U^{4+} ion up to 350 K obtained from the CEF parameters given in the text.

netostriction and ultrasound measurements. Whereas the magnetostriction shows pronounced elongation along the a and c axes and contraction along the b axis, the volume effect at the FOMP is almost zero [Fig. 4(c)]. This strongly suggests that the uranium valence hardly changes across the transition. Therefore, the FOMP is connected with a rotation of a substantially localized uranium magnetic moments from the easy (a) to the hard magnetization direction (b). The localized picture is supported by a large spontaneous magnetic moment, 1.7 μ_B per U atom along the a axis [11]. Nevertheless, the $5f$ states are not fully localized. Their partly itinerant nature is reflected in the high Curie temperature, T_C = 73 K, of $U_3Cu_4Ge_4$ as compared to 7.5 - 23 K of isostructural $R_3Cu_4Ge_4$, where R is a rare-earth element with localized $4f$ states [29–32].

The magnetic structure should not transform across the FOMP. Due to the anisotropic nature of the transition, the whole ferromagnetic structure rotates from the easy to the hard magnetization direction, which preserves its periodicity. Nevertheless, small changes of the Fermi surface are possible due to changes in the lattice dimensions as evidenced by the magnetostriction measurements [Fig. 4(c)].

The elastic response of $U_3Cu_4Ge_4$ to the FOMP may reflect an anisotropic charge distribution of uranium as its magnetic moment rotates from the easy to the hard direction. Multipolar interactions likely play an important role at the FOMP leading to a large softening of the relative sound velocity and large peaks in the sound attenuation [Figs. 4(b) and (d)]. Here, an odd-parity multipole order may be induced. Such an order requires a locally noncentrosymmetric crystal structure, while the underlying crystal structure preserves the inversion symmetry globally [33].

The uranium atoms occupy two crystallographic sites in $U_3Cu_4Ge_4$, $2a$ (U1) and $4j$ (U2) [inset in Fig. 1(a)]. The $2a$ site has mmm symmetry, i.e., there are mirror planes perpendicular to the a, b, and c axes and, therefore, a local inversion center [34]. By contrast, the $4j$ site has $mm2$ symmetry, i.e., there is no mirror plane perpendicular to the c axis. Instead, a screw axis along the c direction is given. Locally, the $4j$ site has no inversion center. Therefore, the uranium atoms in this position might carry an odd-parity multipole order. Multipolar interactions are likely responsible for the large softening of $\Delta v/v$ for C_{44} with decreasing temperature below 200 K as well [Fig. 8(a)].

The elastic moduli reflect the coupling of the strain field to the ultrasonic stress in the presence of electric multipolar moments, which are described by the orbital degrees of freedom of the respective crystal-electric-field (CEF) state. With decreasing temperature, multipolar interactions strengthen, which can be regarded as the multipolar moments attempting to order. This produces a lattice distortion in a way to minimize the coupling between the multipolar moments. The observed elastic softening reflects the lattice distortion.

Quadrupolar degrees of freedom can be described using strain (quadrupolar) susceptibility, $-\chi_{O_\gamma}$, within mean-field theory [17, 35]. Here, O_γ is a quadrupolar operator. The elastic modulus, C_{ii}, is defined by the second-order partial derivative of the total free energy, $F_{\rm total}$, with respect to the strain, ε_i:

$$C_{ii}(T) = \left(\frac{\partial^2 F_{\text{total}}(\varepsilon_i, T)}{\partial \varepsilon_i^2}\right)_{\varepsilon_i \to 0} = \\ = C_{ii}^{(0)}(T) - \frac{N_0 g_i^2 \chi_{O_\gamma}(T)}{1 - g_i' \chi_{O_\gamma}(T)}, \quad (3)$$

where quadrupole-strain and quadrupole-quadrupole interactions are taken into account using the mean-field type inter-site quadrupole-strain, g_i, and quadrupole-quadrupole, g_i', coupling constants, respectively. $N_0 = 1.531 \times 10^{28}$ is the number of U ions per unit volume. $-\chi_{O_\gamma}$ reflects the quadrupolar character of the lowest CEF levels. $C_{ii}^{(0)}$ is the background stiffness. The relative sound-velocity changes can be computed using the relation $\frac{\Delta v}{v} = \frac{\Delta C}{2C}$.

A quantitative analysis of the sound-velocity data is challenging due to the $5f$ electrons being between itinerant and localized. Since the uranium magnetic moment of $U_3Cu_4Ge_4$ is substantially localized, we assume a $5f^2$ state for uranium (U^{4+}) above T_C. For the CEF parameters $B_2^0 = 5$ K, $B_2^2 = 10$ K, $B_4^0 = 2$ K, and $B_4^2 = 10$ K and higher-order parameters equal to zero, we reproduce the softening of $\Delta v/v$ for C_{44} qualitatively as can be seen for $-\chi_{O_{yz}}$ [Fig. 8(b)]. Since our analysis is based on strain-quadrupolar interactions, quadrupolar degrees of freedom are required to explain the observed softening. The broad maximum in C_{44} near 150 K is not reproduced in $\chi_{O_{yz}}$, but probably is caused by a phonon background which is unknown and not taken into account in our calculations.

Based on the abovementioned CEF parameters, we propose the tentative CEF level scheme for $U_3Cu_4Ge_4$ shown in Fig. 8(c). In an orthorhombic CEF, the 9-fold multiplet of U^{4+} splits into 9 singlets. The ground-state singlet Γ_1 is separated from the first excited singlet Γ_4 by 117 K. The second and third excited levels are at 281 and 330 K, respectively. All other CEF levels lie above 2000 K (not shown). The present CEF level scheme explains the origin of the instability in C_{44} with decreasing temperature. The ground-state singlet has no quadrupolar degeneracy and cannot account for the observed softening, i.e., the matrix element $\langle\Gamma_1|O_{yz}|\Gamma_1\rangle$ is zero. The first excited state at 117 K, however, makes an interlevel transition from the ground state possible. This quasi-doublet state has a quadrupolar degeneracy (the matrix element $\langle\Gamma_1|O_{yz}|\Gamma_4\rangle$ is not zero) and explains the softening of C_{44} due to quadrupolar interactions.

The relative sound velocity for C_{33} and C_{55} increases with decreasing temperature in the paramagnetic state [Fig. 8(a)]. Our calculations indicate that the quadrupolar susceptibilities for the operators O_0^2 and O_{zx} are small [Fig. 8(b)], and the experimental results can be explained assuming that the phonon contribution is dominant for C_{33} and C_{55}, respectively. In contrast to C_{44}, no quadrupolar degrees of freedom are required to explain the temperature dependence of $\Delta v/v$ for C_{33} and C_{55}. A reasonable qualitative agreement between experiment and theory for $\Delta v/v$ suggests that the physical properties of $U_3Cu_4Ge_4$ cannot be satisfactorily described by assuming an integer number of f electrons of uranium. This supports the conventional picture of uranium-based intermetallic compounds that the $5f$ states are between fully itinerant and fully localized.

V. SUMMARY

We investigated the elastic response of the uniaxial ferromagnet $U_3Cu_4Ge_4$ to the first-order magnetization process in pulsed fields up to 40 T. We found a pronounced softening in the acoustic modes and peaks in the sound attenuation of longitudinal and transverse acoustic waves across the transition. The crystal lattice elongates along the a and c axes and shrinks along the b axis, producing an almost zero volume effect. This suggests negligible changes in the $5f$ electron localization. Additionally, our analysis of the temperature-dependent sound velocity suggests that the $5f$ states are between fully itinerant and fully localized. The large anomalies observed in the magnetoelastic properties reflect the strong spin-orbit coupling of uranium and crystal-electric-field effects. We also found a Debye-type dispersion of longitudinal acoustic waves, most likely due to rattling motions of the Cu and/or Ge atoms.

VI. ACKNOWLEDGMENTS

We acknowledge the support from the Deutsche Forschungsgemeinschaft (DFG) through the Würzburg-Dresden Cluster of Excellence on Complexity and Topology in Quantum Matter–*ct.qmat* (EXC 2147, Project No. 390858490), as well as the support of the HLD at HZDR, member of the European Magnetic Field Laboratory (EMFL). This work is supported by JSPS KAKENHI Grant Nos. JP21KK004601, Project No. 21-09766S of the Czech Science Foundation, and by MGML (https://mgml.eu) within the Program of Czech Research Infrastructures (Project No. LM2018096).

[1] V. Sechovský and L. Havela, Magnetism of ternary intermetallic compounds of uranium, in *Handbook of Magnetic Materials*, edited by K. H. J. Buschow (Elsevier, Amsterdam, 1998), Vol. 11.

[2] C. Pfleiderer, Superconducting phases of f-electron compounds, Rev. Mod. Phys. **81**, 1551 (2009).

[3] C. Geibel, S. Thies, D. Kaczorowski, A. Mehner, A. Grauel, B. Seidel, U. Ahlheim, R. Helfrich, K. Pe-

tersen, C. D. Bredl, and F. Steglich, A new heavy-fermion superconductor: UNi_2Al_3, Z. Phys. B **83**, 305 (1991).

[4] C. Geibel, C. Schank, S. Thies, H. Kitazawa, C. D. Bredl, A. Böhm, M. Rau, A. Grauel, R. Caspary, R. Helfrich, U. Ahlheim, G. Weber, and F. Steglich, Heavy-fermion superconductivity at $T_c = 2$ K in the antiferromagnet UPd_2Al_3, Z. Phys. B **84**, 1 (1991).

[5] S. S. Saxena, P. Agarwal, K. Ahilan, F. M. Grosche, R. K. W. Haselwimmer, M. J. Steiner, E. Pugh, I. R. Walker, S. R. Julian, P. Monthoux, G. G. Lonzarich, A. Huxley, I. Sheikin, D. Braithwaite, and J. Flouquet, Superconductivity on the border of itinerant-electron ferromagnetism in UGe_2, Nature (London) **406**, 587 (2000).

[6] D. Aoki, A. Huxley, E. Ressouche, D. Braithwaite, J. Flouquet, J.-P. Brison, E. Lhotel, and C. Paulsen, Coexistence of superconductivity and ferromagnetism in URhGe, Nature (London) **413**, 613 (2001).

[7] N. T. Huy, A. Gasparini, D. E. de Nijs, Y. Huang, J. C. P. Klaasse, T. Gortenmulder, A. de Visser, A. Hamann, T. Görlach, and H. v. Löhneysen, Superconductivity on the Border of Weak Itinerant Ferromagnetism in UCoGe, Phys. Rev. Lett. **99**, 067006 (2007).

[8] V. Sechovský, L. Havela, F. R. de Boer, and E. Brück, Magnetic anisotropy in UTX compounds, J. Alloys Compd. **181**, 179 (1992).

[9] V. Sechovský, L. Havela, H. Nakotte, F. R. de Boer, and E. Brück, Anisotropy of magnetism in actinide and lanthanide intermetallics, J. Alloys Compd. **207-208**, 221 (1994).

[10] D. S. Parker, N. Ghimire, J. Singleton, J. D. Thompson, E. D. Bauer, R. Baumbach, D. Mandrus, L. Li, and D. J. Singh, Magnetocrystalline anisotropy in UMn_2Ge_2 and related Mn-based actinide ferromagnets, Phys. Rev. B **91**, 174401 (2015).

[11] D. I. Gorbunov, M. S. Henriques, A. V. Andreev, Y. Skourski, M. Richter, L. Havela, and J. Wosnitza, First-order magnetization process as a tool of magnetic-anisotropy determination: Application to the uranium-based intermetallic $U_3Cu_4Ge_4$, Phys. Rev. B **93**, 064417 (2016).

[12] D. Kaczorowski, H. Noël, and M. Potel, Structural, magnetic and electrical properties of new uranium intermetallics: $U_3Cu_4Si_4$ and $U_3Cu_4Ge_4$, Physica B **206-207**, 457 (1995).

[13] S. Pechev, B. Chevalier, B. Darriet, P. Gravereau, and J. Etourneau, Synthesis and magnetic behaviour of the ternary germanides UCu_2Ge_2 and $U_3Cu_4Ge_4$, J. Alloys Compd. **243**, 77 (1996).

[14] S. Pechev, B. Chevalier, D. Laffargue, B. Darriet, and J. Etourneau, Magnetic structure of the ternary germanide $U_3Cu_4Ge_4$, J. Alloys Compd. **271-273**, 448 (1998).

[15] G. Asti and F. Bolzoni, Theory of first order magnetization processes: Uniaxial anisotropy, J. Magn. Magn. Mater. **20**, 29 (1980).

[16] G. Asti, First-order Magnetic Processes, in *Handbook of Magnetic Materials*, edited by K. H. J. Buschow and E. P. Wohlfarth (Elsevier, Amsterdam, 1990), Vol. 5.

[17] B. Lüthi, *Physical Acoustics in the Solid State* (Springer, Heidelberg, 2005).

[18] S. Zherlitsyn, S. Yasin, J. Wosnitza, A. A. Zvyagin, A. V. Andreev, and V. Tsurkan, Spin-lattice effects in selected antiferromagnetic materials, Low Temp. Phys. **40**, 123 (2014).

[19] R. Daou, F. Weickert, M. Nicklas, F. Steglich, A. Haase, and M. Doerr, High resolution magnetostriction measurements in pulsed magnetic fields using fiber Bragg gratings, Rev. Sci. Instrum. **81**, 033909 (2010).

[20] A. Tamaki, T. Goto, S. Kunii, M. Kasaya, T. Suzuki, T. Fujimura, and T. Kasuya, Elastic Properties of SmB_6 and Sm_3Se_4, J. Magn. Magn. Mater. **47&48**, 469 (1985).

[21] T. Goto, Y. Nemoto, K. Sakai, T. Yamaguchi, M. Akatsu, T. Yanagisawa, H. Hazama, K. Onuki, H. Sugawara, and H. Sato, Quadrupolar effect and rattling motion in the heavy-fermion superconductor $PrOs_4Sb_{12}$, Phys. Rev. B **69**, 180511(R) (2004).

[22] I. Ishii, Y. Suetomi, T. K. Fujita, K. Suekuni, T. Tanaka, T. Takabatake, T. Suzuki, and M. A. Avila, Lattice instability and elastic dispersion due to the rattling motion in the type-I clathrate $Ba_8Ga_{16}Sn_{30}$, Phys. Rev. B **85**, 085101 (2012).

[23] T. Goto, Y. Nemoto, K. Sakai, T. Yamaguchi, M. Akatsu, T. Yanagisawa, H. Hazama, and K. Onuki, Quadrupolar effect and rattling motion in the heavy-fermion superconductor $PrOs_4Sb_{12}$, Phys. Rev. B **69**, 180511(R) (2004).

[24] T. Yanagisawa, Y. Ikeda, H. Saito, H. Hidaka, H. Amitsuka, K. Araki, M. Akatsu, Y. Nemoto, T. Goto, P.-C. Ho, R. E. Baumbach, and M. B. Maple, Magnetic-Field-Independent Ultrasonic Dispersions in the Magnetically Robust Heavy Fermion System $SmOs_4Sb_{12}$, J. Phys. Soc Jpn. **80**, 043601 (2011).

[25] Y. Nemoto, T. Yamaguchi, T. Horino, M. Akatsu, T. Yanagisawa, T. Goto, O. Suzuki, A. Dönni, and T. Komatsubara, Ferroquadrupole ordering and Γ 5 rattling motion in the clathrate compound $Ce_3Pd_{20}Ge_6$, Phys. Rev. B **68**, 184109 (2003).

[26] T. Yanagisawa, P.-C. Ho, W. M. Yuhasz, M. B. Maple, Y. Yasumoto, H. Watanabe, Y. Nemoto, and T. Goto, Ultrasonic Investigation of Off-Center Rattling in Filled Skutterudite Compound $NdOs_4Sb_{12}$, J. Phys. Soc. Jpn. **77**, 074607 (2008).

[27] K. Suekuni, M. A. Avila, K. Umeo, H. Fukuoka, S. Yamanaka, T. Nakagawa, and T. Takabatake, Simultaneous structure and carrier tuning of dimorphic clathrate $Ba_8Ga_{16}Sn_{30}$, Phys. Rev. B **77**, 235119 (2008).

[28] It is likely that the field-independent anomalies observed in $\Delta v/v$ and $\Delta\alpha$ for the acoustic mode C_{44} around 20 K [Figs. 2(b) and (e)] have a similar origin as for C_{33}. Unfortunately, ultrasound measurements at frequencies above 17.1 MHz were challenging due to the strong attenuation for this acoustic mode.

[29] S. K. Dhar, S. Singh, P. Bonville, C. Mazumdar, P. Manfrinetti, and A. Palenzona, Magnetic behavior of $Yb_3Cu_4Ge_4$ and $Gd_3Cu_4Ge_4$, Physica B **312-313**, 846 (2002).

[30] A. Szytuła, E. Wawrzyńska, B. Penc, N. Stüsser, and A. Zygmunt, Magnetic properties of $R_3Cu_4X_4$ (R = Gd-Er; X = Ge, Sn) compounds, Physica B **327**, 167 (2003).

[31] E. Wawrzyńska, J. Hernandez-Velasco, B. Penc, A. Szytuła, and A. Zygmunt, Magnetic structures of $R_3Cu_4Ge_4$ (R=Tb, Dy, Ho, Er), J. Magn. Magn. Mater. **264**, 192 (2003).

[32] K. Katoh, M. Maeda, S. Matsuda, and A. Ochiai, Magnetic and transport properties of single-crystal $Yb_3Cu_4Ge_4$, J. Magn. Magn. Mater. **324**, 2914 (2012).

[33] H. Watanabe and Y. Yanase, Group-theoretical classification of multipole order: Emergent responses and candidate materials, Phys. Rev. B **98**, 245129 (2018).

[34] *International Tables for Crystallography*, edited by Th. Hahn (Springer, Dordrecht, 2005), Vol. A.

[35] T. Yanagisawa, H. Matsumori, H. Saito, H. Hidaka, H. Amitsuka, S. Nakamura, S. Awaji, D. I. Gorbunov, S. Zherlitsyn, J. Wosnitza, K. Uhlířová, M. Vališka, and V. Sechovský, Electric Quadrupolar Contributions in the Magnetic Phases of UNi_4B, Phys. Rev. Lett. **126**, 157201 (2021).